

THE MEAN IMPULSE RESPONSE OF HOMOGENEOUS ISOTROPIC TURBULENCE: THE FIRST (DNS-BASED) MEASUREMENT

Marco Carini* and Maurizio Quadrio*

*Dipartimento di Ingegneria Aerospaziale
Politecnico di Milano, Campus Bovisa, Via La Masa 34, 20156 Milano, Italy
e-mail: maurizio.quadrio@polimi.it, web page:
<http://www.aero.polimi.it/~quadrio>

Keywords: Homogeneous isotropic turbulence, statistical closure theories, impulse response measurement, DNS, DIA, LET.

Abstract. *A DNS-based measurement of the mean impulse response function for stationary homogeneous isotropic turbulence (HIT) is proposed and carried out here for the first time. A zero-mean white-noise volume forcing is used to probe the turbulent flow and the response function is obtained by accumulating the space-time correlation between the white forcing and the velocity field. The interest of this research lies in the crucial role played by the mean impulse response of HIT in the context of renormalized perturbation closure theories, starting from the Direct Interaction Approximation (DIA) theory of Kraichnan. Measuring (through a DNS numerical experiment) the actual measured response enables us for the first time to compare it with the available theoretical predictions.*

A computer code has been developed and equipped with parallel (SMP) computing capabilities specifically to carry out this research. Even though our results are still limited to relatively low values of the Reynolds number Re_λ , a preliminary analysis is however possible. Very good agreement is obtained with the Kraichnan's picture of random convection effects, both in terms of time scaling and of characteristic form of the response function. Further work is needed to establish whether random convection dominance still affects the response behavior in presence of a well-developed inertial range of scales, i.e. at higher Re_λ .

1 INTRODUCTION

The concept of *impulse response tensor* of a turbulent flow lies at the heart of the Direct Interaction Approximation (DIA) theory, developed 50 years ago [8] by the great theoretical physicist Robert Kraichnan, to tackle the turbulence closure problem analytically. Since then, along the theoretic path of *renormalized perturbations*, several closures have been proposed such as the Local Energy Transfer (LET) theory introduced by McComb [16], and eventually within a Lagrangian framework, as done by Kraichnan himself [10, 11] and others [3, 6]. In all such theories, either Eulerian or Lagrangian, closure is achieved by means of a closed set of integro-differential equations, where the unknowns are the two-points, two-times velocity correlation tensor and the response tensor itself. (An exception is LET where a propagator tensor plays the role of the response tensor.) In general, the equations of motion after closure must be solved numerically: the only analytical, although approximate, solution has been derived by Kraichnan for the response tensor from DIA equations form in the case of HIT.

During the last decades, comparison between the *true* HIT statistics and the corresponding theoretical predictions has been carried out by means of DNS at increasing values of Re_λ and available experimental data, in the stationary as well as in the freely decaying regime. Encouraging results both for LET theory and Lagrangian closures have been reported [17, 18, 5, 6]. Up to the present day, however, the comparison between the calculated and the actual response function has never been addressed, due to the complete lack of experimental information about it. However this is not a minor issue at all for closure theories: as stressed by McComb in Ref. [17], the differences among the various theoretical approaches rely upon the form of the response or propagator equation, whereas the covariance equation is most often treated in equivalent ways.

In recent years Luchini *et al.* in Ref. [14] have proposed a method to carry out the Eulerian DNS-based measurement of the mean impulse response of a turbulent flow, and have described the response function of a fully developed turbulent channel flow to small-amplitude perturbations applied at the wall. Due to lack of isotropy, this response tensor is quite complicated, and does not directly relate to the previous theories, since it was conceived in the framework of turbulence control (hence the emphasis on wall flows and wall forcing), where it is achieving its first results (see for example Ref. [?], to be presented at this same Conference). The measurement technique proposed in [14], however, provides us with the required tools to obtain the impulse response tensor for HIT, where volume forcing has to be considered.

Describing the response function in the simpler framework of HIT is the goal of the present work. The knowledge of the response function could pave an original way to improve our understanding of turbulence dynamics, and looking at it in HIT, where only non-linear dynamics among scales is present, is a perfectly suited starting point. This paper intends therefore to describe the measurement of the Eulerian HIT response, presenting preliminary results, obtained at low values of Re_λ , that enable us to analyze the characteristic form of the response and its characteristic scales, and to compare them with theoretical predictions.

The paper is organized as follows. In the next §2, the required theoretical background is briefly reviewed, with special focus on the DIA theory. The DNS-based measurement technique is described in §3, where the numerical procedure is validated against the available analytical viscous solution, and accuracy considerations are discussed. In §4 the actual response function in HIT is presented and compared with the theoretical predictions. Lastly, section 5 is devoted to a concluding discussion.

2 THE THEORETICAL BACKGROUND

The method of renormalized perturbations, to which belong all the abovementioned closure theories, was first developed in quantum mechanics to tackle the well-known many-body problem [15], which is common to several fields of physics. In this problem, where strong non-linear interactions couple the whole set of degrees of freedom, the convergence of truncated power series in the appropriate scale parameter – i.e. the Reynolds number in turbulence – cannot be achieved. Hence the failure of traditional small perturbations methods, that are limited to the case of weak interactions only. In extreme synthesis, the fundamental idea at the roots of renormalized perturbation theory is to rewrite the above *bare expansions* by means of series partial summations over infinite terms (with the aid of Feynman diagrams) or by means of reversion of functional power series. In both cases, the approximate results turn out not to suffer from strong non-linear interactions.

Due to the complexity of the analytical tools required, in the following sections we will limit ourselves to describing the statistical homogeneous isotropic form of the DIA closure equations, by underlying its main achievements and drawbacks.

The starting point is the statement of Navier-Stokes Equations (NSE) in wave-vector space:

$$\left(\frac{\partial}{\partial t} + \nu\kappa^2\right) u_i(\boldsymbol{\kappa}, t) = M_{ijm}(\boldsymbol{\kappa}) \int u_j(\mathbf{p}, t) u_m(\boldsymbol{\kappa} - \mathbf{p}, t) d\mathbf{p} + P_{ij}(\boldsymbol{\kappa}) f_j(\boldsymbol{\kappa}, t), \quad (1)$$

where $u_i(\boldsymbol{\kappa}, t)$ is the Fourier coefficient of the i -component of the velocity field, function of time t and wavevector $\boldsymbol{\kappa}$, $P_{ij}(\boldsymbol{\kappa}) = \delta_{ij} - \kappa^{-2}\kappa_i\kappa_j$ is the projection tensor in Fourier space, and the third order tensor $M_{ijm}(\boldsymbol{\kappa}) \equiv -i/2(\kappa_m P_{ij}(\boldsymbol{\kappa}) + \kappa_j P_{im}(\boldsymbol{\kappa}))$ is introduced as a shorthand. Lastly, $\mathbf{f}(\boldsymbol{\kappa}, t)$ denotes an external stirring body force, i.e. the energy-driving force in the isotropic stationary case, which is assumed as prescribed in statistical terms. Since the closure will be obtained at second order in the hierarchy of the statistical moments, the mean correlation tensor of the turbulent velocity field is introduced directly in its spectral form:

$$Q_{ij}(\boldsymbol{\kappa}, t, t') = \langle u_i(\boldsymbol{\kappa}, t) u_j(-\boldsymbol{\kappa}, t') \rangle, \quad (2)$$

where the notation $\langle \cdot \rangle$ indicates the ensemble averaging operator. In the homogeneous isotropic case considered here, the tensor function Q_{ij} boils down to a scalar function \widehat{Q} :

$$Q_{ij}(\boldsymbol{\kappa}, t, t') = P_{ij}(\boldsymbol{\kappa}) \widehat{Q}(\kappa, t, t'), \quad (3)$$

where $\kappa = \|\boldsymbol{\kappa}\|$. If stationarity is assumed, the time dependence reduces only to temporal separation, $\tau = t - t'$, leading to the simplest form $Q(\kappa, \tau)$ for the correlation function:

$$Q(\kappa, \tau) = \widehat{Q}(\kappa, t, t - \tau). \quad (4)$$

2.1 The definition of the impulse response function

Following Sagaut and Cambon [21], the most general definition of the instantaneous impulse response tensor of a turbulent velocity field $\mathbf{u}(\boldsymbol{\kappa}, t)$ with respect to an external volume force $\mathbf{f}(\boldsymbol{\kappa}, t)$, is given in terms of the following input-output relation between infinitesimal perturbations, $\delta(\cdot)$ (note the different notation from the Dirac's delta function $\delta(\cdot)$):

$$\delta u_i(\boldsymbol{\kappa}, t) = \int \int_{-\infty}^t H_{in}(\boldsymbol{\kappa}, \boldsymbol{\kappa}', t, t') \delta f_n(\boldsymbol{\kappa}', t') dt' d\boldsymbol{\kappa}'. \quad (5)$$

It is essential to realize that the perturbation has a *stochastic meaning*, in the sense that it is performed around a particular random realization of \mathbf{u} which is itself solution of the fully nonlinear NSE in Fourier space. Therefore $H_{in}(\boldsymbol{\kappa}, \boldsymbol{\kappa}', t, t')$ has a random nature, and an integral formulation not only in time but also in wave-vector space is required. In fact the instantaneous response tensor has the meaning of a *tangent Green's function* related to a *random and nonlinear* state, satisfying the instantaneous response equation:

$$\begin{aligned} \left(\frac{\partial}{\partial t} + \nu \kappa^2 \right) H_{in}(\boldsymbol{\kappa}, \boldsymbol{\kappa}', t, t') = \\ = 2M_{ijm}(\boldsymbol{\kappa}) \int u_j(\mathbf{p}, t) H_{mn}(\boldsymbol{\kappa} - \mathbf{p}, \boldsymbol{\kappa}', t, t') d\mathbf{p} + P_{in}(\boldsymbol{\kappa}) \delta(\boldsymbol{\kappa} - \boldsymbol{\kappa}') \delta(t - t'), \end{aligned} \quad (6)$$

which is derived from a *stochastic Green function formalism* applied to the linearized form of Eq. (1). The response tensor *locality in wave-vector space* follows only after averaging:

$$\langle H_{in} \rangle = \mathcal{H}_{in}(\boldsymbol{\kappa}, t, t') \delta(\boldsymbol{\kappa} - \boldsymbol{\kappa}'). \quad (7)$$

As for the correlation tensor, exploiting statistical isotropy and stationarity results in scalar response functions, respectively $\widehat{\mathcal{G}}$ and \mathcal{G} , defined as follows:

$$\mathcal{H}_{in}(\boldsymbol{\kappa}, t, t') = P_{in}(\boldsymbol{\kappa}) \widehat{\mathcal{G}}(\kappa, t, t'), \quad (8)$$

$$\mathcal{G}(\kappa, \tau) = \mathcal{G}(\kappa, t, t - \tau). \quad (9)$$

The causality property holds for both the previous functions, hence:

$$\widehat{\mathcal{G}}(\kappa, t, t') = 0 \quad \text{for } t \leq t' \text{ and } \forall \kappa. \quad (10)$$

This is obviously a consequence of the realizability of the dynamical system to which the response belongs. Moreover as indicated by Kraichnan in Ref. [8], the scalar response is a *real function* which is unit bounded:

$$|\mathcal{G}(\kappa, \tau)| \leq \mathcal{G}(\kappa, 0^+) = 1, \quad \forall \tau > 0 \text{ and } \forall \kappa. \quad (11)$$

This is not surprising, since unit scale factor for delta functions implicitly appears in Eq. (6), and the various contributions to the response cannot be more in phase than they are at zero time separation.

2.2 The Direct Interaction Approximation

Even though the original statement of DIA theory, presented by Kraichnan in Ref. [8], was not explicitly based on renormalized perturbations theory, several such methods have been successful since then in re-deriving the DIA equations: the recent review of Kaneda [4] summarizes up to 8 different ways of doing that. In fact, as observed by McComb [17], the renormalization framework seems to better support DIA theory rather than the original Kraichnan's hypothesis, on a theoretically rigorous base. As a consequence, this interpretation of the DIA has become the leading one among researchers. The renormalized derivation of DIA has been given by Wyld [22] with the use of Feynman diagrams. Instead the easiest, though not completely self-explanatory, way in which DIA equations can be derived is found in the classical textbooks by

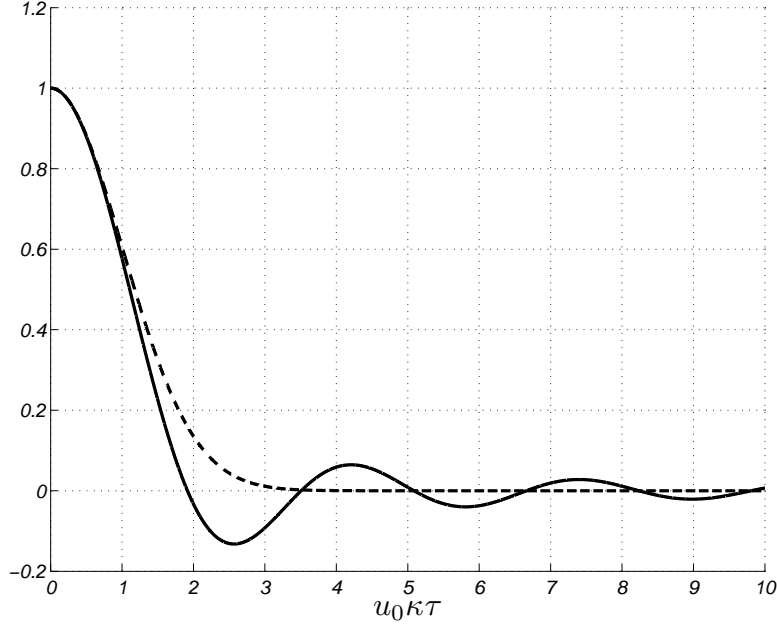


Figure 1: Turbulent-diffusive part of DIA's analytical response (—) and Gaussian-convective response $\exp(-1/2u_0^2\kappa^2\tau^2)$ (---), see §2.3.

Leslie [13] and by McComb [17]. Starting from power series expansions of both the correlation and the response function, the following closure equations are obtained:

$$\left\{ \begin{array}{l} \left(\frac{\partial}{\partial t} + \nu\kappa^2 \right) \widehat{\mathcal{G}}(\kappa, t, t') = - \int L(\boldsymbol{\kappa}, \mathbf{p}) \left[\int_{t'}^t \widehat{\mathcal{G}}(\mathbf{p}, t, s) \widehat{\mathcal{G}}(\kappa, s, t') \widehat{\mathcal{Q}}(\|\boldsymbol{\kappa} - \mathbf{p}\|, t, s) ds \right] d\mathbf{p} + \\ \quad + \delta(t - t'), \\ \left(\frac{\partial}{\partial t} + \nu\kappa^2 \right) \widehat{\mathcal{Q}}(\kappa, t, t') = \int L(\boldsymbol{\kappa}, \mathbf{p}) \left[\int_{-\infty}^{t'} \widehat{\mathcal{G}}(\kappa, t', s) \widehat{\mathcal{Q}}(\mathbf{p}, t, s) \widehat{\mathcal{Q}}(\|\boldsymbol{\kappa} - \mathbf{p}\|, t, s) ds + \right. \\ \quad \left. - \int_{-\infty}^t \widehat{\mathcal{G}}(\mathbf{p}, t, s) \widehat{\mathcal{Q}}(\|\boldsymbol{\kappa} - \mathbf{p}\|, t, s) \widehat{\mathcal{Q}}(\kappa, t', s) ds \right] d\mathbf{p} + \int_{-\infty}^{t'} \widehat{\mathcal{G}}(\kappa, t', s) \widehat{\mathcal{F}}(\kappa, t, s) ds. \end{array} \right. \quad (12)$$

Here $L(\boldsymbol{\kappa}, \mathbf{p})$ denotes a scalar function (with geometric meaning) that takes the following form:

$$L(\boldsymbol{\kappa}, \mathbf{p}) = \frac{[\alpha(\kappa^2 + p^2) - \kappa p(1 + 2\alpha^2)](1 - \alpha^2)\kappa p}{\kappa^2 + p^2 - 2\kappa p\alpha}, \quad (13)$$

where α is the cosine of the angle between $\boldsymbol{\kappa}$ and \mathbf{p} ; see Refs. [13] and [17] for further details. At the same time $\widehat{\mathcal{F}}(\kappa, t, t')$ is the scalar counterpart of the volume force correlation tensor in the homogeneous isotropic case:

$$\langle f_i(\boldsymbol{\kappa}, t) f_j(-\boldsymbol{\kappa}, t') \rangle = \mathcal{F}_{ij}(\boldsymbol{\kappa}, t, t') = P_{ij}(\boldsymbol{\kappa}) \widehat{\mathcal{F}}(\kappa, t, t'), \quad (14)$$

which is assumed prescribed.

Starting from the system (12), Kraichnan obtained the following approximate solution for the mean impulse response function:

$$\mathcal{G}(\kappa, \tau) = \exp(-\nu\kappa^2\tau) \frac{J_1(2u_0\kappa\tau)}{u_0\kappa\tau}, \quad (15)$$

where u_0 indicates the r.m.s. of the fluctuating turbulent field, and J_1 is the Bessel function of the first kind. The inviscid part of Kraichnan's analytical solution is illustrated in Fig. 1. What might surprise at first sight is that at each scale κ the time decay of the response function is dominated by the local energy-range time scale, $(u_0\kappa)^{-1}$, and this remains true even when κ belongs to the universal range of scales. From analytical investigation of the DIA equations at statistical equilibrium, Kraichnan indeed derived an inertial power law exponent of $-3/2$ for the energy spectrum in the inertial subrange. This deviation from the well-established Kolmogorov $-5/3$ law is due to an energy cascade that, though local in wave-number space, is regulated by the energy-containing scales, and not by the viscous scales as required by the first similarity hypothesis of the Kolmogorov K41 theory [7]. In particular the analysis by Edwards reported in [13] highlights that a true Kolmogorov scaling is embedded in the covariance equation, but not in the response equation, since its wave-number integral is singular for $\kappa \rightarrow 0$ if Kolmogorov scaling is assumed. In deriving the above form of the response function, Kraichnan indeed introduced a fixed lower cutoff on the integration wave-number domain, located at the boundary of the energy-containing range. Only by introducing an *ad hoc* lower cutoff that is variable and proportional to κ , Kolmogorov scaling can be restored, thus correcting *a posteriori* the original formulation of the DIA equations.

2.3 The Postulate of Random Galilean Invariance and Eulerian closures

A Random Galilean Invariance (RGI) postulate was introduced by Kraichnan in 1964 [9] to explain the failure of DIA in yielding the Kolmogorov inertial-range scaling. At the same time, related arguments provided a rationale for a further reworking of the closure theories, that were translated into the more cumbersome Lagrangian form, thus overcoming the difficulties implied by the Eulerian formulation of the equations.

The RGI postulate is a statistical restatement of the well-known deterministic Galilean invariance principle that is at the roots of classical mechanics. In its stochastic form, the space-time uniform relative velocity between two observers becomes a random vector with *zero mean*, that changes its orientation and magnitude in each realization of the stochastic system, according to a prescribed statistical distribution, such as the common Gaussian one. Kraichnan argued that turbulent statistics of all order which are simultaneously computed, i.e. at zero time separation, must be *invariant with respect to the Galilean random group* of transformations. In particular this is important when modeling third-order correlations which are known to be associated with energy transfer among scales, and which appear in the energy spectrum equation in their simultaneous form. In fact the DIA closure results in the approximation of the abovementioned simultaneous triple correlations with non-simultaneous forms of \hat{Q} and \hat{G} . As a consequence, the RGI requirement is not satisfied, and spurious effects in the relaxation process of third-order moments are introduced, that lead to a local time scaling belonging to the energy-containing range. This explains why the energy transfer along the energy cascade is regulated by the level of excitation at low wave numbers, thus causing the deviation from the Kolmogorov spectrum in the inertial subrange.

In the Kraichnan's analysis, violating RGI is equivalent to a picture where the undistorted sweeping effect of the largest eddies over the smallest ones dominates the relaxation process of the Eulerian response and correlation functions over the whole range of scales. This effect of *random convection* on the temporal scaling of the response function can be illustrated by means of an idealized convection problem (described in Ref. [9]) of the form:

$$\frac{\partial \mathbf{u}}{\partial t} = -i\boldsymbol{\kappa} \cdot \mathbf{v}\mathbf{u}(\boldsymbol{\kappa}, t), \quad (16)$$

where $\mathbf{u}(\boldsymbol{\kappa}, t)$ is a random fluctuating velocity field, resembling turbulence fluctuations, convected by a uniform constant velocity \mathbf{v} , that randomly varies from realization to realization of \mathbf{u} , with $\|\mathbf{u}\| \ll \|\mathbf{v}\|$. Assuming that at the initial time the two variables are statistically independent¹ with a normal distribution, the exact Eulerian response function can be shown to be equal to $\widehat{\mathcal{Q}}(\boldsymbol{\kappa}, t, t')$, with the following analytic expression:

$$\widehat{\mathcal{G}}(\boldsymbol{\kappa}, t, t') = \widehat{\mathcal{Q}}(\boldsymbol{\kappa}, t, t') = \exp\left(-\frac{1}{2}v_0^2\boldsymbol{\kappa}^2(t-t')\right), \quad \text{with } t > t', \quad (17)$$

where v_0 is the r.m.s. value of the \mathbf{v} distribution. Eq. (16) can be considered as a simplified form of the NSE, where both viscous and non-linear terms in \mathbf{u} are neglected. Extending the previous result to the fully turbulent case, the turbulent Eulerian response is likely to be affected by a spurious diffusive behavior due to the random convection of the large eddies over smaller eddies, without distortion of the former. Following this analogy, v_0 in Eq. (17) assumes the meaning of the r.m.s. of turbulent fluctuations, and turbulent Gaussian convective response will be written as:

$$\mathcal{G}(\boldsymbol{\kappa}, \tau) = \exp\left(-\frac{1}{2}u_0^2\boldsymbol{\kappa}^2\tau\right), \quad \text{with } \tau > 0. \quad (18)$$

In Fig. 1 the Gaussian convective response is shown together with the DIA response solution. The two functions overlap for $\tau u_0 \boldsymbol{\kappa} \ll 1$, as happens for the so-called *random oscillator* model problem when a Gaussian behavior is assumed: in this case, as illustrated in Ref. [13] and [4], the exact solution takes the same form of Eq. (18) and the comparison with the DIA approximation as shown in Fig. 1 still holds. Also from this example it is evident that oscillations in the DIA solution are rather unphysical: as pointed out by Kraichnan himself, a monotone behavior should be observed.

More recently McComb *et al.* started a discussion [19] on the relevance of the RGI postulate and the limits of Eulerian approach to the closure problem. They argued that, for a properly constructed ensemble of transformations to inertial frames, RGI is implied by invariance in every realization both of NSE and of the relations among statistical moments that are derived from them. A new invariance requirement into statistical mechanics is therefore not required, since RGI follows as a corollary of deterministic Galilean invariance. At the same time numerical integration of both DIA and LET equations, carried out in the range $0.5 \leq Re_\lambda \leq 1009$ for freely decaying HIT, appears to question the predicted dominance of convective scaling in both the response and the correlation function. Numerical evidence indicates that convective scaling is effective at low Re_λ , $Re_\lambda \leq 4.5$, but Kolmogorov scaling begins to be effective at $Re_\lambda \approx 40$ and becomes the proper scaling at $Re_\lambda \approx 1000$, when a wide inertial range of scales is clearly developed. However, the latest papers on the subject by McComb and coworkers come back to their own previous analysis with renewed criticism, owing to new results in the stationary forced regime and due to a reworking of LET equations. Ref. [20] shows that LET theory, which is the only Eulerian closure leading to the Kolmogorov scaling in the inertial range, can be rewritten only in terms of single point, single time functions due to the property of the propagator, and this may possibly reconcile LET behavior with Kraichnan's analysis.

As an intermediate conclusion, the investigations of McComb and coworkers definitely raise some questions about the actual behavior of the response function. Such questions are addressed by numerical experiments as the ones proposed in this paper.

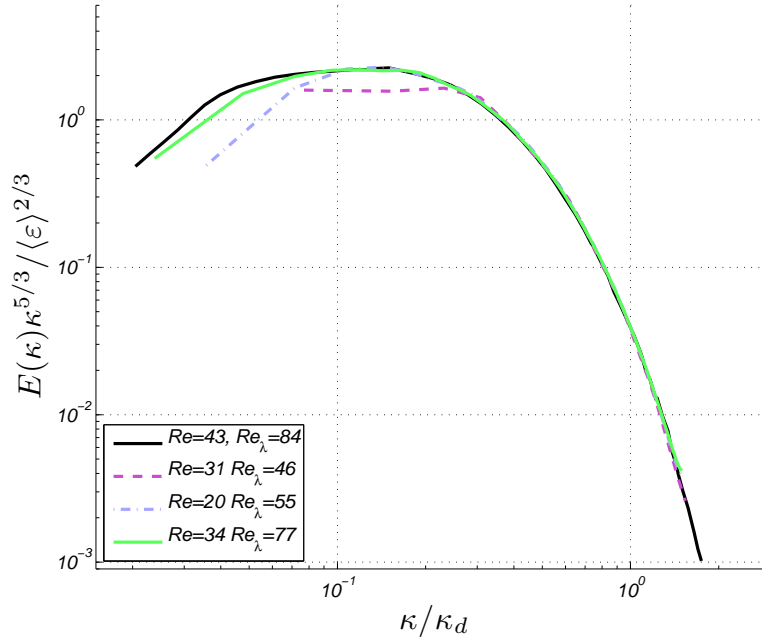


Figure 2: Comparison of compensated energy spectrum for HIT: computed $E(\kappa)$ for several Re values are shown together with the spectrum taken from Ref. [12] at $Re_\lambda = 84$ (black line).

3 MEASURING THE RESPONSE FUNCTION BY DNS

The measurement of \mathcal{G} described in this paper is carried out by means of a forced DNS of stationary HIT on a cubic domain, whose edge length L is chosen to be $L = 2\pi$ for convenience so that $\kappa_0 = 2\pi/L = 1$ without loss of generality. A numerical code has been developed on purpose and equipped with parallel (shared-memory) computing capabilities. The code implements a traditional Galerkin-Fourier scheme applied to the velocity-vorticity formulation of the incompressible Navier-Stokes equations. Exact removal of the aliasing error is obtained with the 3/2 zero-padding rule; time integration is performed by means of a third-order low-storage Runge-Kutta (Williamson) scheme; see Ref. [1] for additional numerical details. The forcing scheme has been carefully implemented following the provisions stated in Ref. [12], the notation of which is used here. The Kolmogorov scale is indicated with η , with $\kappa_d = \eta^{-1}$, the instantaneous dissipation rate is ε , the forcing-containing shell is κ_f and the mean energy injection rate is P , that equals $\langle \varepsilon \rangle$ at statistical stationarity. A standard resolution of $\kappa_{max}\eta = 1.5$ is adopted, where κ_{max} indicates the maximum resolved wave-number in each direction of the Fourier space. The code has been tested by simulating standard forced HIT, and by comparing its results to the energy spectra published in Ref. [12], at several values of Re_λ . A comparison of this kind is shown in Fig 2, that shows excellent agreement between computed and published.

3.1 The response measurement technique

In Ref. [14] Luchini, Quadrio & Zuccher have proposed an innovative method for measuring the impulse response of a turbulent velocity field, resorting to the statistical statement of the input-output relation for a linear system, i.e. the input-output correlation. This approach is primarily motivated by the problem of low signal-to-noise ratio (S/N), since impulsive perturbations, externally introduced in the turbulent field to measure its response, must be small

¹At later times the two velocity vectors are no longer statistically independent.

compared to turbulent fluctuations for linearity implied by Eq. (5) to hold.

When dealing with the stochastic response of a linear system, a fundamental mathematical tool is represented by the *white-noise process*. It is well known from filtering theory [2] that when a linear system is fed by a white noise, the correlation between the input and the output is proportional to the impulse response of the system, owing to the delta-correlated property of the white-noise input. We employ here an independently generated random volume forcing as the input; by computing its cross-correlation with the velocity field, the whole wave-number dependency of the response function is obtained at once. At the same time forcing is uniformly distributed over time and space, thus leading to larger amplitude within the linearity constraint. Therefore the proposed method is much better than a deterministic forcing, be it either periodic or impulsive, which would lead to unaffordable simulations, as stressed in Ref. [14].

Starting from Eq. (5), the input-output correlation can be written as:

$$\begin{aligned} \langle \delta u_i(\boldsymbol{\kappa}, t) \delta f_j(-\boldsymbol{\kappa}, t - \tau) \rangle &= \\ &= \int \int_{-\infty}^{+\infty} \mathcal{H}_{in}(\boldsymbol{\kappa}, t - t') \delta(\boldsymbol{\kappa}' - \boldsymbol{\kappa}) \langle \delta f_n(\boldsymbol{\kappa}', t') \delta f_j(-\boldsymbol{\kappa}', t - \tau) \rangle dt' d\boldsymbol{\kappa}', \end{aligned} \quad (19)$$

where Eq. (7) has been used owing to the average operator, and the response causality property allows the extension towards $+\infty$ of the upper bound of time integral. Assuming $\delta f_i(\boldsymbol{\kappa}, t) = \epsilon w_i(\boldsymbol{\kappa}, t)$, with ϵ scale factor and $w_i(\boldsymbol{\kappa}, t)$ independently generated zero-mean white-noise signal with identity covariance matrix, one has:

$$\langle \delta f_n(\boldsymbol{\kappa}', t') \delta f_j(-\boldsymbol{\kappa}', t - \tau) \rangle = \delta_{nj} \delta(t' - t + \tau), \quad (20)$$

and the cross-correlation at the l.h.s. of Eq. (19) will result in the properly scaled response tensor:

$$\langle \delta u_i(\boldsymbol{\kappa}, t) \delta f_j(-\boldsymbol{\kappa}, t - \tau) \rangle = \epsilon^2 \mathcal{H}_{ij}(\boldsymbol{\kappa}, \tau). \quad (21)$$

We shall denote by $\tilde{\mathbf{u}}(\boldsymbol{\kappa}, t)$ the turbulent velocity field when volume forcing with white signal is applied. If the perturbation is small enough for linearity to hold, i.e. $\epsilon \ll 1$, it follows that:

$$\tilde{\mathbf{u}}(\boldsymbol{\kappa}, t) = \mathbf{u}_\epsilon(\boldsymbol{\kappa}, t) + \delta \mathbf{u}(\boldsymbol{\kappa}, t), \quad (22)$$

where $\mathbf{u}_\epsilon(\boldsymbol{\kappa}, t)$ indicates a different realization of the turbulent fluctuating field respect to the original field $\mathbf{u}(\boldsymbol{\kappa}, t)$, as a consequence of non-linearity and stochastic behavior of NSE. Then computing the correlation between $\tilde{\mathbf{u}}$ and $\delta \mathbf{f}$ results in:

$$\frac{\langle \tilde{u}_i(\boldsymbol{\kappa}, t) \delta f_j(-\boldsymbol{\kappa}, t - \tau) \rangle}{\epsilon^2} = \frac{1}{\epsilon^2} [\langle u_{\epsilon i}(\boldsymbol{\kappa}, t) \delta f_j(-\boldsymbol{\kappa}, t - \tau) \rangle + \langle \delta u_i(\boldsymbol{\kappa}, t) \delta f_j(-\boldsymbol{\kappa}, t - \tau) \rangle]. \quad (23)$$

Since the applied random perturbation on forcing is uncorrelated to turbulent fluctuations, the term $\langle u_{\epsilon i}(\boldsymbol{\kappa}, t) \delta f_j(-\boldsymbol{\kappa}, t - \tau) \rangle$ will be averaged out in the previous equation, leading to:

$$\frac{\langle \tilde{u}_i(\boldsymbol{\kappa}, t) \delta f_j(-\boldsymbol{\kappa}, t - \tau) \rangle}{\epsilon^2} = \mathcal{H}_{ij}(\boldsymbol{\kappa}, \tau), \quad (24)$$

where the input-output correlation law, Eq. (19), has been used to handle the non vanishing term at r.h.s. of Eq. (23). In this way it is still possible to measure the turbulent response using the cross-correlation between the white-noise input and the whole turbulent velocity field. As a last observation, in the HIT case Eq. (8) provides us with a convenient way of accumulating just the scalar version of the response function, by means of shell averaging over tensor trace:

$$\oint \mathcal{H}_{ii}(\boldsymbol{\kappa}, \tau) dS(\boldsymbol{\kappa}) = 8\pi \kappa^2 \mathcal{G}(\kappa, \tau). \quad (25)$$

3.2 The purely viscous Stokes' response: validation of the measurement procedure

The Stokes or *viscous* response represents the zero-order term in the expansion series of \mathcal{G} as introduced in the context of renormalized perturbations. The Stokes response, $\mathcal{G}^{(0)}$, can be easily derived from Eq. (6) after removal of the non-linear terms, thus providing the solution for pure viscous dynamics of the velocity field. Its analytical form reads:

$$\mathcal{G}^{(0)}(\kappa, \tau) = \exp(-\nu\kappa^2\tau). \quad (26)$$

It is important to notice that the Stokes response has a *deterministic* nature, due to the linearity of the Stokes operator: Kraichnan usually refers to it as “*statistically sharp*”. The exact solution for the Stokes case provides an useful tool for the validation of the full measurement procedure. To this purpose, the Stokes response can be also retrieved from a DNS of the fully non-linear NSE through a *numerical linearization*. In this way the algorithm to be employed for the true measurement in the turbulent case is unchanged, but a null initial condition is adopted, the simulation is not forced, and only the white-noise perturbation is applied. If $\epsilon \ll 1$, no evolution to turbulence dynamics is produced, and non-linear terms $\mathcal{O}(\epsilon^2)$ are negligible respect to linear ones $\mathcal{O}(\epsilon)$ which define the Stokes equation.

The Stokes response has been measured in numerical experiments with a spatial resolution of 32^3 modes (with aliasing), mainly to keep small the computational cost which is obviously the same as in the turbulent case. Table 1 summarizes the discretization parameters employed for the measurement of the response function; they are the forcing amplitude ϵ , the number of stored time correlations N_c , their time separation $\Delta\tau$, and the averaging time T_{av} .

A comparison between the exact response and its point-wise measures in the (κ, τ) plane is illustrated in Fig. 3. It demonstrates good agreement between the measured and the exact solution. Global accuracy tests have been conducted using the L^2 norm of the local error $\mathcal{E}(\kappa, \tau) = \mathcal{G}^{(0)}(\kappa, \tau) - \mathcal{G}_m^{(0)}(\kappa, \tau)$:

$$\|\mathcal{E}\|_{L^2(\mathbb{D}_m)} = \left(\frac{1}{D_m} \int_{\mathbb{D}_m(\kappa, \tau)} \mathcal{E}^2(\kappa, \tau) d\kappa d\tau \right)^{1/2}, \quad (27)$$

where $\mathbb{D}_m \equiv [1, \kappa_{max}] \times [0, N_c\Delta\tau]$ indicates the time-wave-number range covered in the (κ, τ) plane with area D_m . A piece-wise linear interpolation of measured data is used to perform the above integral. A linear dependence with respect to ϵ , as well as with respect to the delta-correlation time resolution $\Delta\tau$ is confirmed by the $\|\mathcal{E}\|_{L^2(\mathbb{D}_m)}$ trends of Fig.4. Similarly, from the same figure one sees that the error due to average over finite time interval scales approximately with order $-1/2$, as expected from central limit theorem and ergodicity. In the analysis of the global order of accuracy, the asymptotic behavior, due to all the different contributions, has been removed to emphasize the interested trend alone. In Fig. 5 (top and center) the time decay of the Stokes response at $\kappa/\kappa_0 = 8$ is plotted: convergence to the exact solution at small time separations (compared to local viscous time scale $(\tau\nu\kappa^2)^{-1}$) is obtained with smaller time steps employed for the discretization of the white noise delta correlation, $\Delta\tau$. In the same figure (bottom), the measured Stokes response plotted at different wave numbers correctly shows a collapse (within the accuracy limits) when local viscous time scaling is adopted for $\Delta\tau$.

4 RESULTS

Several DNS runs have been carried out to measure the impulse response of the turbulent flow in the HIT setting: Table 2 summarizes the discretization parameters adopted for each

<i>Run</i>	N_c	$\Delta\tau\nu\kappa_{max}^2$	ϵ	$T_{Av}\nu\kappa_0^2$
1	50	9.172E-3	1E-3	0.91720
2	50	9.172E-3	1E-3	9.1720
3	50	9.172E-3	1E-3	91.720
4	50	4.586E-2	1E-3	0.91720
5	50	4.586E-2	1E-3	9.1720
6	50	4.586E-2	1E-3	91.720
7	50	4.586E-2	1E-3	910.20
8	50	9.172E-2	1E-3	0.91720
9	50	9.172E-2	1E-3	9.1720
10	50	9.172E-2	1E-3	91.720
11	50	9.172E-2	1E-3	910.20
12	50	2.293E-1	1E-3	0.91720
13	50	2.293E-1	1E-3	9.1720
14	50	2.293E-1	1E-3	91.720
15	50	4.586E-1	1E-3	0.91720
16	50	4.586E-1	1E-3	9.1720
17	50	4.586E-1	1E-3	91.720
18	50	4.586E-2	5E-4	91.720
19	50	4.586E-2	1E-3	91.720
20	50	4.586E-2	5E-3	91.720
21	50	4.586E-2	1E-2	91.720

Table 1: Discretization parameters for the Stokes response measurements, with 32^3 modes (with aliasing), $\Delta\tau = \Delta t$ and $\kappa_{max}/\kappa_0 = 10$.

N	κ_{max}/κ_0	κ_d/κ_0	P	κ_f/κ_0	$Re = \left(\frac{\kappa_d}{\kappa_f}\right)^{4/3}$	Re_λ	$u_0 \left(\frac{\kappa_f}{P}\right)^{1/3}$
64	20	13	1	1	31	46	1.4635
128	42	28	1	3	20	55	1.7862
192	63	42	1	3	34	77	1.8453

Table 2: Parameters and results of reference for performed HIT DNS.

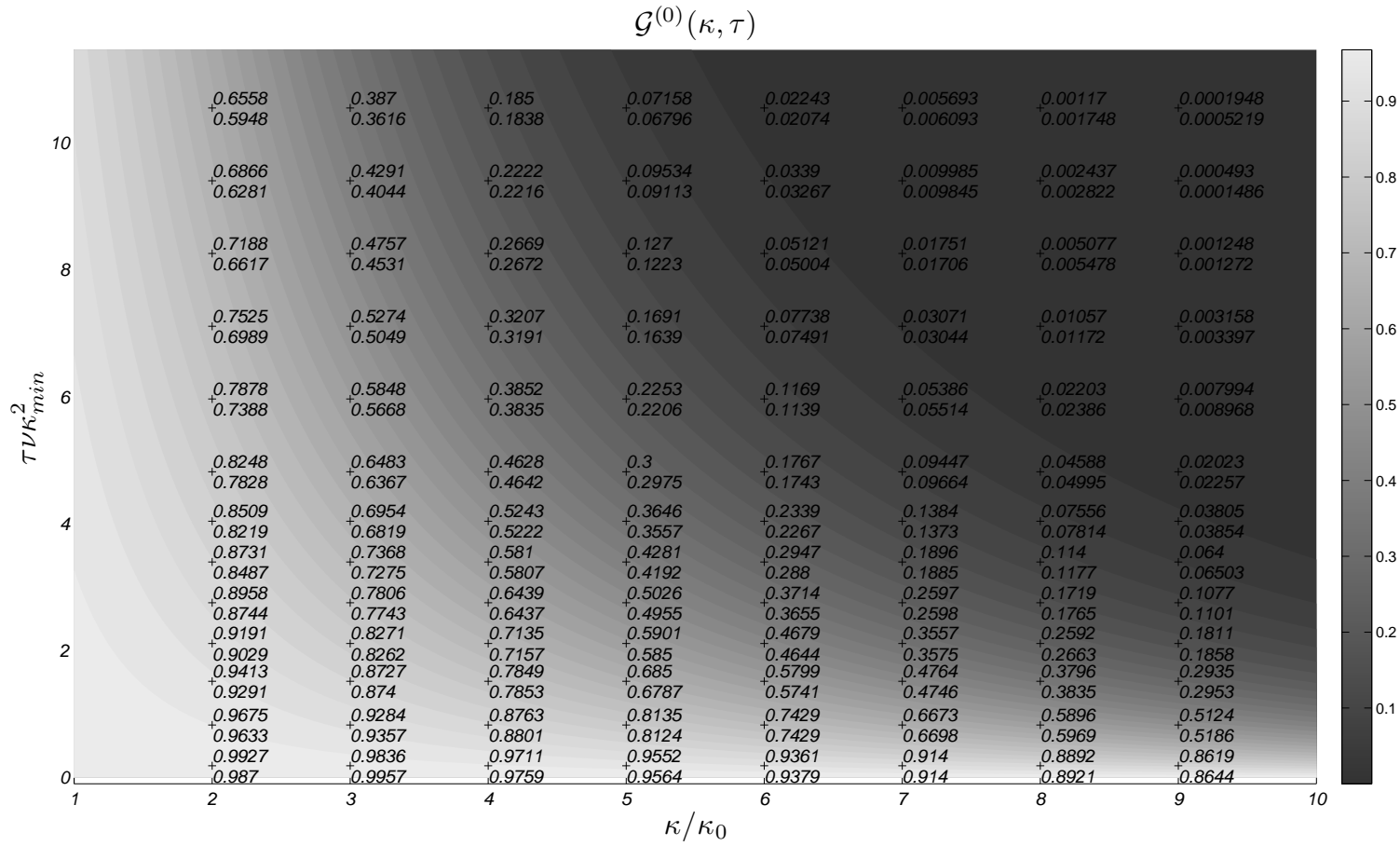


Figure 3: Comparison between the analytical Stokes response and the measured one at some of the available measure points: at each measure point (+) the top value refers to the analytic exact solution and bottom value is the measured one.

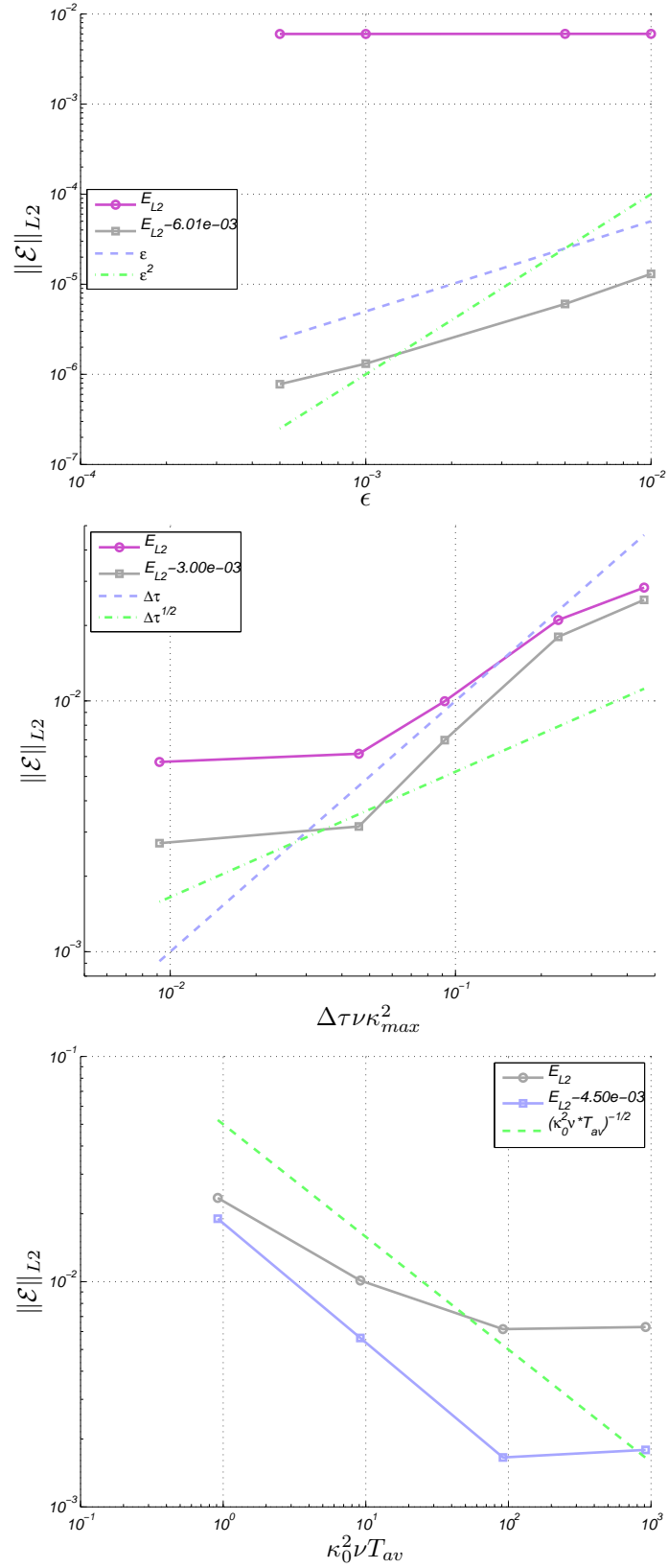


Figure 4: Trends of $\|\mathcal{E}\|_{L^2(\mathbb{D}_m)}$ respect to the measurement parameters. Top: linear order of accuracy respect to ϵ . Center: linear order of accuracy respect to $\Delta\tau$. Bottom: trend of $\|\mathcal{E}\|_{L^2(\mathbb{D}_m)}$ respect to the the scaled averaging time $\kappa_0^2 \nu T_{av}$.

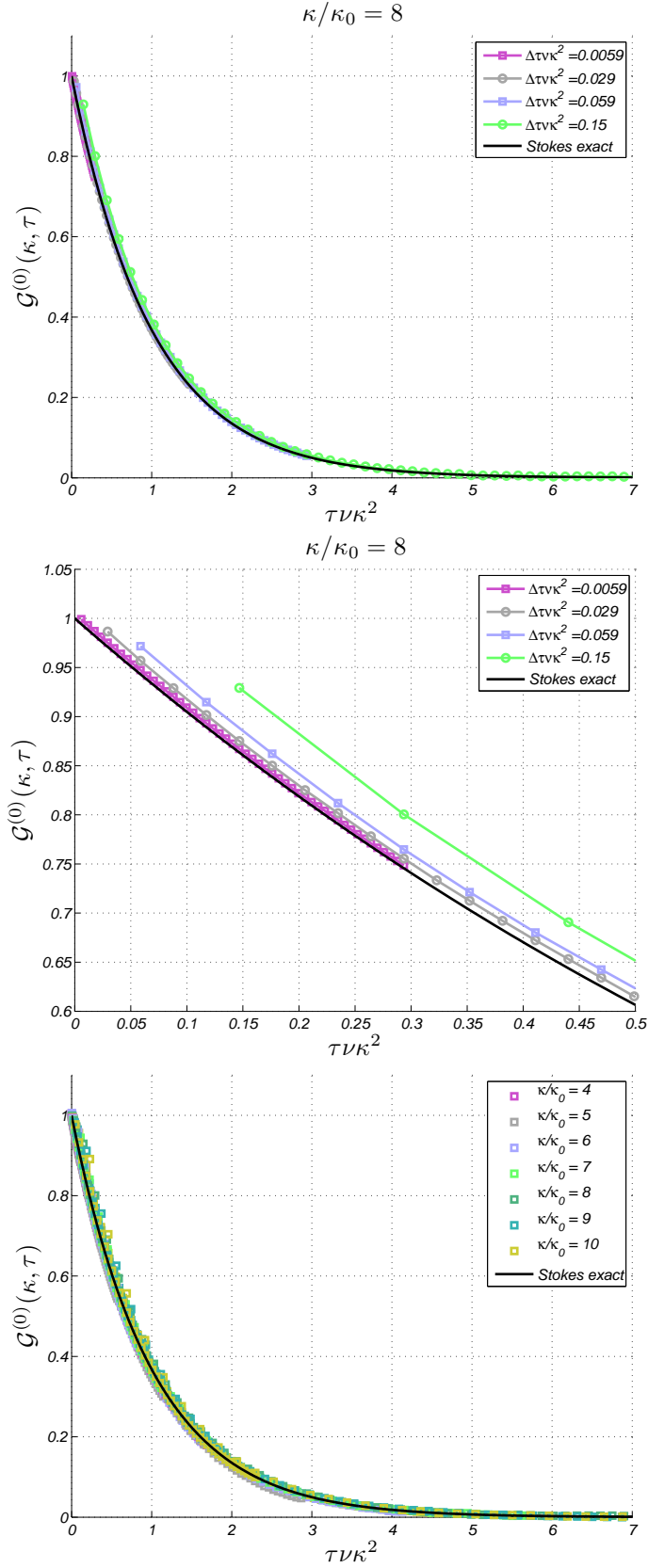


Figure 5: Time decay of measured $\mathcal{G}^{(0)}$ at different $\Delta \tau$. Top: comparison between the measured and exact Stokes response at fixed $\kappa/\kappa_0 = 8$. Center: zoom for $\tau \nu \kappa^2 \ll 1$. Bottom: Stokes response at several wave number κ/κ_0 vs. non-dimensional time separation $\tau \nu \kappa^2$, emphasizing collapse.

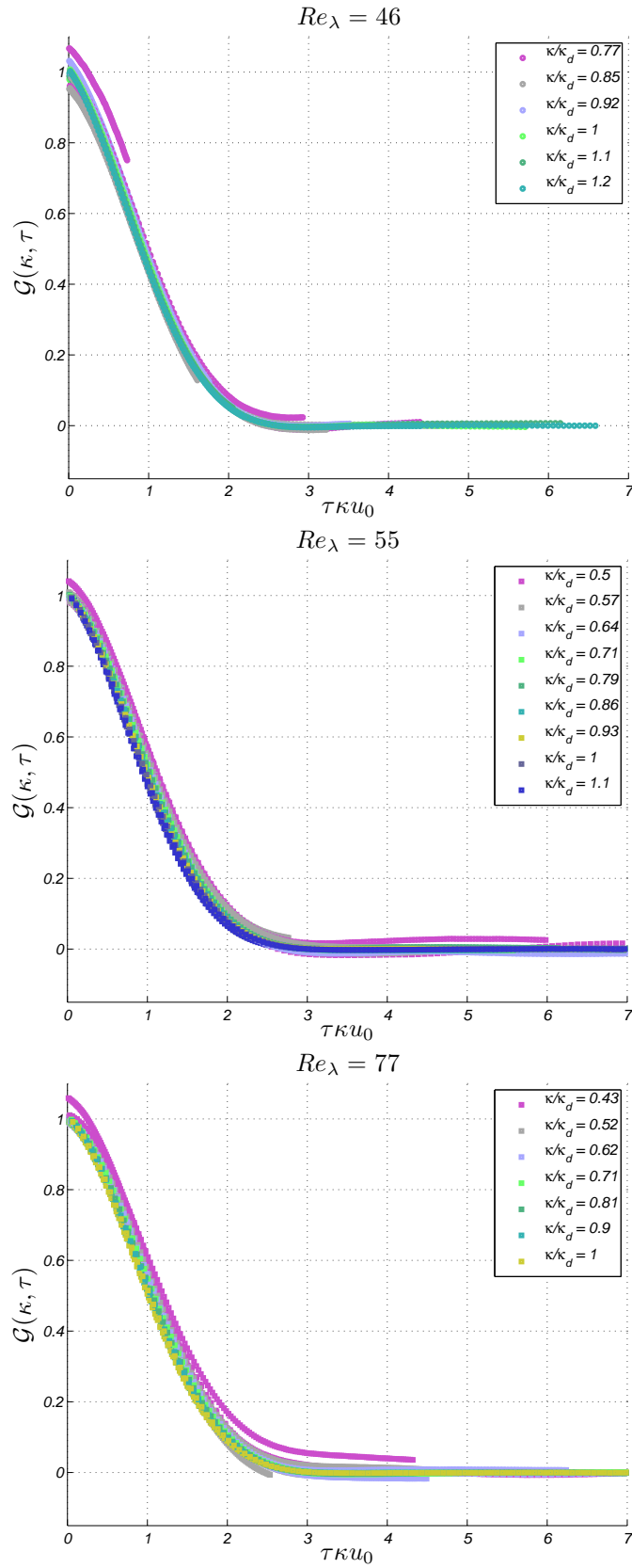


Figure 6: The measured turbulent response vs. non-dimensional time separation $\tau u_0 \kappa$, for several wavenumbers in the universal dissipative subrange. Top: $Re_\lambda = 46$. Center: $Re_\lambda = 55$. Bottom: $Re_\lambda = 77$.

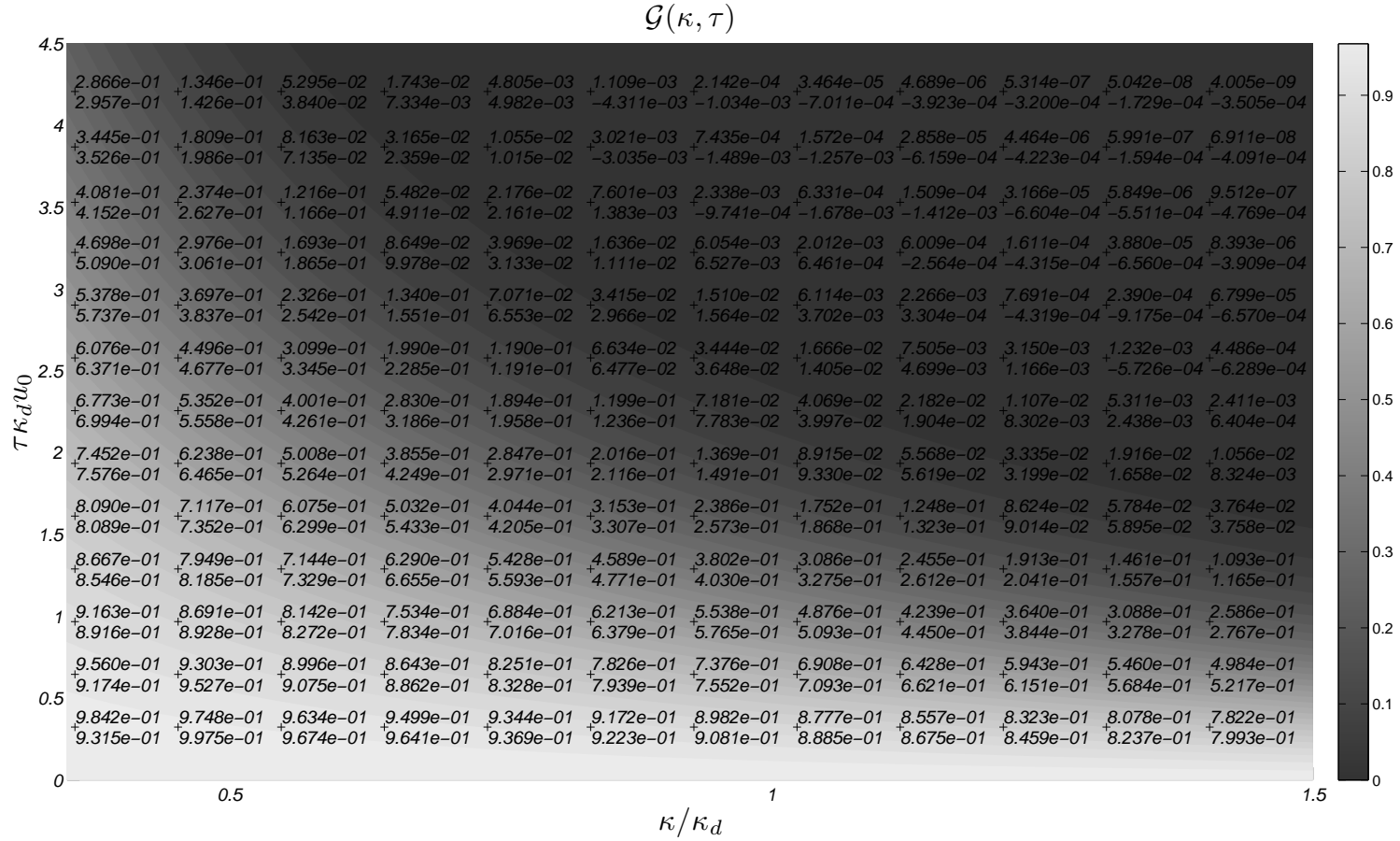


Figure 7: Comparison between viscous Gaussian-convective solution $\mathcal{G}(\kappa, \tau) = \exp(-\nu\kappa^2\tau - 1/2u_0^2\kappa^2\tau^2)$ and the measured response at some of the available measure points for $Re_\lambda = 77$: at each point (+) top value refers to the previous analytic formula while bottom value is the measured one.

N	Re_λ	Run	N_c	$\Delta\tau u_0 \kappa_d$	ϵ	$T_{Av} u_0 \kappa_d$	$N_{Core} (SMP)$	$Comp. time [h]$
64	46	1	100	0.0571	0.005	1712.3	2	3.4
		2	100	0.0381	0.005	1141.5	2	3.4
		3	100	0.0190	0.005	570.77	2	3.4
		4	100	0.0095	0.005	285.39	2	3.4
128	55	1	150	0.1595	0.0038	5583	4	46.7
		2	150	0.0798	0.0038	2791.5	4	46.7
		3	150	0.0520	0.0038	1820.5	4	46.7
		4	150	0.0322	0.0038	1128.7	4	46.7
192	77	1	150	0.2418	0.0033	8463.8	8	89.4
		2	150	0.1397	0.0033	4890.2	8	89.4
		3	150	0.0672	0.0033	2351	8	89.4
		4	150	0.0484	0.0033	1692.8	8	89.4
		5	150	0.0322	0.0033	1128.5	8	89.4

Table 3: Discretization parameters for the DNS-based measurement of the HIT response function.

DNS resolution, whereas Table 3 lists all the simulations that led to response measurements, together with the discretization parameters pertaining to the response function. Given the available computational resources, the values of Re_λ are low or moderate, ranging from $Re_\lambda = 46$ to $Re_\lambda = 77$.

In Fig. 6 an assessment of the convective scaling of the turbulent response is provided, limited to the universal viscous subrange of scales. The apparent small deviations that are observed at the lower wave numbers are due to residual time-averaging error, and could be removed by employing a longer simulation time. Fig. 8 offers a more detailed comparison between the available analytical response, provided by Kraichnan’s analysis, and the measured one at $\kappa = \kappa_d$, i.e. at the Kolmogorov scale, and at $Re_\lambda = 55$. At time separations smaller than the local energy time scale, i.e. $\tau u_0 \kappa < 1$, the response is in very good agreement with the DIA response formulae and the viscous Gaussian-convective solution. This latter result does not come as a surprise: even though the turbulent field is non-Gaussian, at times smaller than the characteristic correlation time the Gaussian approximation is still good, see [13]. The unexpected result is that the Gaussian convective solution still approximates very well the measured response at larger times, whereas the DIA solution deviates from it. This is also documented by Fig. 7, where point-wise measurements in the (κ, τ) plane for the universal dissipative range are reported together with the viscous Gaussian-convective analytical function. Only near to the exponential-tail region, i.e. for $\tau u_0 \kappa \approx 3$, the measured response appears to deviate from the Gaussian solution, with the former decreasing faster than the latter.

5 CONCLUSIONS

The impulse response function of homogeneous isotropic turbulence has been measured via DNS and described in some detail. The measurement method has been validated by computing

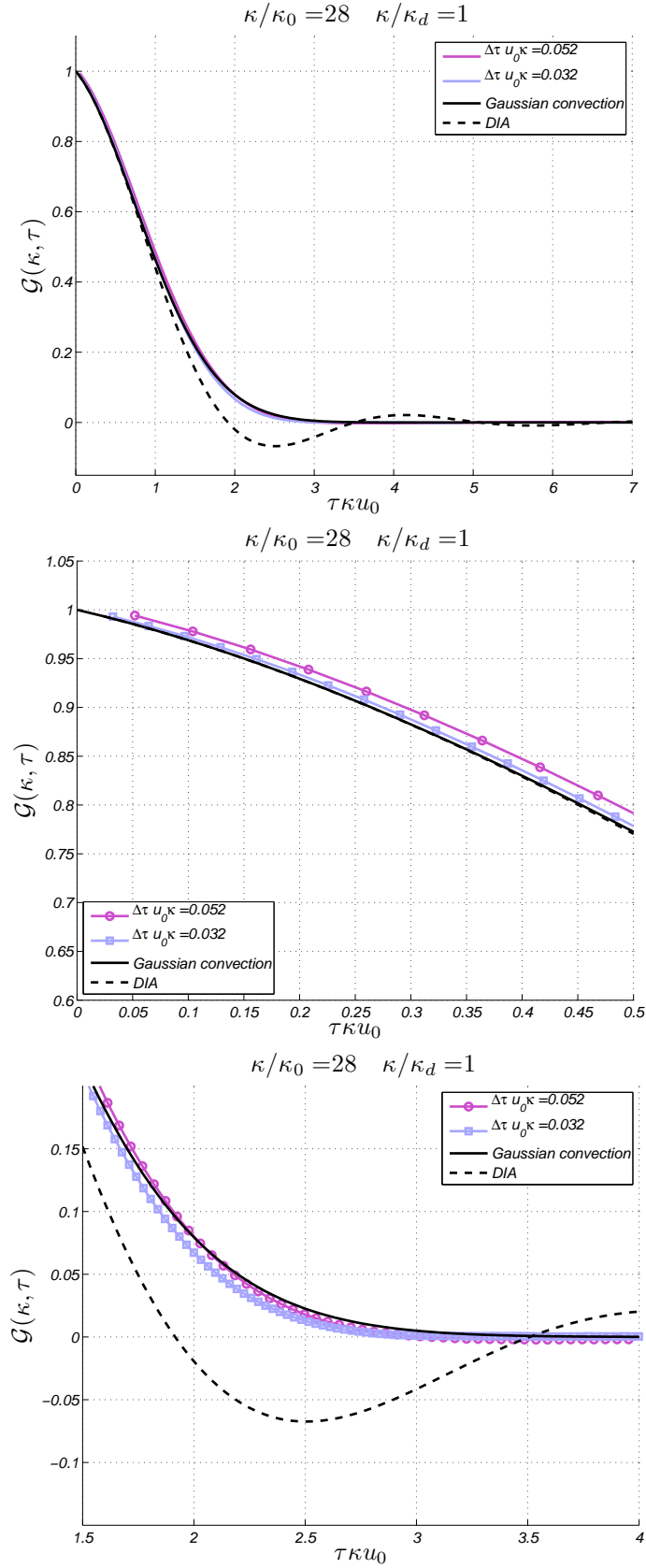


Figure 8: Measured response for runs at $Re_\lambda = 55$. Top: the whole response time decay at Kolmogorov scale compared with DIA and viscous Gaussian-convective solution. Center: a zoom of the picture on the top for $\tau u_0 \kappa \ll 1$. Bottom: a zoom of the picture on the top in the near exponential-tail region.

the same quantity for purely viscous dynamics, for which an analytical solution is available. Based on this test case, the order of accuracy with respect to several discretization parameters has been assessed and shown to follow the expected trends. The proposed methodology has then proved to be effective in the quantitative description of the response behavior within the universal equilibrium range of scales. The analysis in the universal dissipative range confirms the theoretical prediction of energetic-range scaling of the response, and establish such scaling as the dominant one, at least in the range of Re_λ considered here. A somewhat surprising result is that the solution provided by Kraichnan in Ref. [9] to the problem of idealized convection, described in §2.3, shows an extremely good fit to the measured response function, with deviations limited to the near exponential-tail region. This implies that the large-scale fluctuations can be interpreted rightfully as a near-Gaussian field. However, more accurate measurements are required to reliably describe the deviation from Gaussianity, owing to the unavoidable residual error due to finite averaging time.

A more thorough description of the response function and of its relevant time scales obviously calls for an extension of this study to higher values of Re_λ , to reach at least where a well-defined inertial range develops. When such data will be available, the fundamental question about a possible vanishing of convective scaling in favor of Kolmogorov scaling could be properly answered, thus enlightening the current controversial about Eulerian approach to the closure problem. If Kolmogorov scaling should indeed be recovered at higher Re_λ , then the local relaxation processes of the turbulent response would be captured. This would open a new scenario in turbulence modeling, leading to a class of response-based turbulence models that might offer the substantial advantage of being free from adjustable empirical parameters, since more turbulence physics would be contained into the response-based description.

6 ACKNOWLEDGMENTS

The authors would like to thank Dr. Fulvio Martinelli for suggesting the Stokes test case described in §3.2 and for helpful discussions. We gratefully acknowledge the use of the computing system located at the University of Salerno and the discussions with Professor Paolo Luchini.

REFERENCES

- [1] C. Canuto and M. Y. Hussaini. *Spectral Methods - Fundamentals in single domains*. Springer, 2006.
- [2] A. H. Jazwinski. *Stochastic processes and Filtering Theory*. Academic Press, New York, 1970.
- [3] Y. Kaneda. Renormalized expansions in the theory of turbulence with the use of the lagrangian position function. *J. Fluid Mech.*, 107:131–145, 1981.
- [4] Y. Kaneda. Langragian renormalized approximation of turbulence. *Fluid Dyn. Res.*, 39:526–551, 2007.
- [5] Kaneda Y. Lagrangian and eulerian time correlations in turbulence. *Phys. Fluids*, 5:2835–2845, 1993.
- [6] S. Kida and S. Goto. A lagrangian direct-interaction approximation for homogeneous isotropic turbulence. *J. Fluid Mech.*, 345:307–345, 1997.

- [7] A.N. Kolmogorov. The Local Structure of Turbulence in an Incompressible Viscous Fluid for Very Large Reynolds Numbers. *Dokl. Akad. Nauk. SSSR*, 30:301–305, 1941. (Reprinted in Proc. R. Soc. London A v.434 pp.9–13, 1991).
- [8] Kraichnan R. H. The structure of isotropic turbulence at very high reynolds numbers. *J. Fluid Mech.*, 5:497–543, 1959.
- [9] Kraichnan R. H. Kolmogorov hypotheses and eulerian turbulence theory. *Phys. of Fluids*, 7:1723–1734, 1964.
- [10] Kraichnan R. H. Lagrangian-history closure approximation for turbulence. *Phys. of Fluids*, 7:575–598, 1964.
- [11] Kraichnan R.H. Eulerian and lagrangian renormalization in turbulence theory. *J. Fluid Mech.*, 83:349–374, 1977.
- [12] A. G. Lamorgese, D. A. Caughey, and S. B. Pope. Direct numerical simulation of homogeneous turbulence with hyperviscosity. *Phys. of Fluids*, (17), 2005.
- [13] Leslie D. C. *Developments in The Theory of Turbulence*. Clarendon Press, Oxford, 1973.
- [14] P. Luchini, M. Quadrio, and S. Zuccher. Phase-locked linear response of a turbulent channel flow. *Phys. Fluids*, 18(121702):1–4, 2006.
- [15] R. D. Mattuck. *A Guide to Feynman Diagrams in the Many-Body Problem*. Dover Publications, 1992.
- [16] W.D. McComb. A local energy-transfer theory of isotropic turbulence. *J. Phys. A: Math. Nucl. Gen.*, 7:632, 1974.
- [17] W.D McComb. *The Physics of Fluid Turbulence*. Oxford University Press, 1990.
- [18] W.D. McComb, M. J. Filipiak, and V. Shanmugasundaram. Rederivation and further assessment of the let theory of isotropic turbulence, as applied to passive scalar convection. *J. Fluid Mech.*, 245:279–300, 1992.
- [19] W.D. McComb, V. Shanmugasundaram, and P. Hutchinson. Velocity-derivative skewness and two-time velocity correlations of isotropic turbulence as predicted by let theory. *J. Fluid Mech.*, 208:91–114, 1989.
- [20] M. Oberlack, W.D. McComb, and A.P. Quinn. Solution of functional equations and reduction of dimension in the local energy transfer theory of turbulence. *Phys. Rev. E*, 63:026308–1, 2001.
- [21] P. Sagaut and C. Cambon. *Homogeneous Turbulence Dynamics*. Cambridge University Press, 2008.
- [22] Wyld H. W. Formulation of the theory of turbulence in an incompressible fluid. *Ann. Phys.*, 14:143–165, 1961.